https://doi.org/10.1016/j.ress.2023.109599

Resilience-driven post-disaster restoration of interdependent infrastructure systems under different decision-making environments

Min Xu[a], Guoyuan Li[a], Anthony Chen[a,b,*]

Abstract: Critical infrastructure systems are highly interconnected and mutually dependent for smooth functioning. Such interdependencies contribute to operational efficiency but may also exacerbate the negative impacts caused by disruptions, as the failure of one system could spread to its connected systems. To enhance the resilience of interdependent infrastructure systems, this article investigates the post-disaster restoration decision problem and considers two decision-making environments. Firstly, a deterministic restoration decision model is developed under certainty to seek a combined repair sequence that can maximize the resilience of the interdependent system. This model assumes that the decision-makers have perfect information about the restoration decision problem. Then, this article extends this deterministic model to a two-stage stochastic restoration model under uncertainty, in which the repair time of damaged components is assumed to be random and represented by a set of scenarios. A heuristic method, composed of a selection principle and a matrix-based approach, is proposed to solve these two restoration decision models. Numerical experiments on interdependent systems demonstrate that integrating interdependency into the restoration decision problem could significantly benefit system resilience. The developed restoration decision models and heuristic method could provide essential insights into the restoration process of interdependent infrastructure systems.

Keywords: Critical infrastructure system; interdependency; resilience; restoration decision problem; decision-making environments

* Corresponding Author, Email address: anthony.chen@polyu.edu.hk (A. Chen)
[a] Department of Civil and Environmental Engineering, The Hong Kong Polytechnic University, Hong Kong, China
[b] The Hong Kong Polytechnic University Shenzhen Research Institute, Shenzhen 518040, China

1. Introduction

Urban social and economic activities are highly contingent on critical infrastructure service provision, including electricity, potable water, gas, and communication [1,2]. Critical infrastructure systems (CISs) are mutually interdependent for operation and management [3,4]. Electric power systems provide electricity to metro trains and communication devices; utility tunnels (carrying electricity lines, water, and sewer pipes) are generally underground along the road. Unfortunately, such interdependencies also increase the fragility of these systems. The failure of one system could propagate to the other, triggering catastrophic cascading failures [5,6]. The Northeast blackout of 2003 caused 50 million people without power and led to the suspension of trains and airports and the shutdown of communication devices [7]. Currently, the interdependencies across infrastructures are ever-increasing and various types of disasters are becoming more frequent and intense. Infrastructures face growing infrastructure challenges in preserving continuous and stable services [8,9]. Over the past decade, governments and scholars worldwide have called for building resilient CISs to respond to various hazards. Resilience here describes the ability of a system to resist and absorb possible disturbances and quickly recover from them. Proactive protection and restoration actions are the two main approaches to realizing this target [10,11].

Although protection actions could alleviate the adverse effects of disaster events, efficient repair decisions are still indispensable. Protection actions include but are not limited to reinforcing critical components, replacing aging components, and adding redundancy [12-14]. Fang and Zio [15] developed a two-stage robust optimization model to enhance the resilience of interdependent critical infrastructure systems (ICIS) under natural hazards. Reinforcing components and deploying distributed generation units are considered in their study. However, most physical components of CISs are exposed to the earth's surface or buried in the shallow surface, and some of them (i.e., substations and pipes) are pretty sensitive to disturbances. Component failures are

almost inevitable, particularly for extreme natural disasters [16,17]. Meanwhile, restoration resources are usually limited after a significant disruption, which spells that damaged components cannot be repaired simultaneously and immediately. Efficient repair plans are needed to guide the restoration actions and quickly restore system functionality to the pre-disaster level [18,19]. To this end, this article focuses on the post-disaster restoration decision problem of ICISs from the resilience perspective, incorporating interdependencies across them.

The post-disaster restoration decision problem of a single CIS has been wildly studied, and fruitful achievements have been made in the literature. Researchers mainly concentrate on restoration modeling and optimization problems [20,21]. The restoration process is immensely complex, containing various tasks, uncertainties, and preferences [22]. A typical restoration process generally involves inspection, repair, and testing [23, 24]. The sources of uncertainty mainly arise from the state of components, the repair time, the available restoration resources, and dynamic demands [25-27]. The diversity of preferences reflects the requirement of different stakeholders, such as governments, enterprises, nonprofit organizations, and residents [28,29]. Also, a variety of approaches have been adopted to model the restoration process, including network-based, agent-based, Markov process-based, and statistical-based methods [30-32]. Network-based methods are always integrated with optimization techniques to formulate restoration optimization models. These models are categorized into single- or multiple-objective in terms of the involved preferences [22,33] and deterministic or stochastic depending upon the concern of decision-making environments [30,34]. As the restoration decision problems of CISs are NP-hard (non-deterministic polynomial-time hardness), these mathematical models cannot be figured out within a limited time under major disruptions [35,36]. Therefore, researchers have developed various solutions to produce feasible and efficient restoration decisions: importance-based method [37-39], meta-heuristic algorithms [40,41], and principles [42,43]. The importance of a component to the system could be measured by component types (e.g.,

generator and substation), topological characteristics (i.e., degree and betweenness), and the impact on system functionality. Meta-heuristic algorithms, such as genetic and simulated annealing algorithms, can provide optimal or near-optimal solutions for restoration decision problems. The original restoration decision models could be relaxed or simplified by applying various principles. Nurre et al. [35] proposed a novel heuristic dispatching rule for the restoration decision problem of CISs. This dispatching rule selects a path from the source nodes to the demand nodes and repairs the damaged components on this path. Also, this path chosen could bring the most significant benefit to system performance.

The interdependencies across CISs make their restoration decision problems more sophisticated. CISs are highly mutually dependent in complex ways, and the interdependencies can be roughly classified into four categories: physical, cyber, geographical, and logical [3]. These interdependencies are modeled by agent-based [44], system dynamic-based [45], economic theory-based [46], and network-based approaches [47]. Based on four network-based methods proposed in the literature, Mao and Li [48] conducted a comprehensive study to investigate and analyze the impact of interdependencies on the resilience of ICISs. This study indicated that the interdependencies among CISs significantly impact the level of resilience in the context of disaster risk reduction.

Additionally, for different types of interdependencies, researchers have established varied restoration decision models to maximize the resilience of ICISs against various disruptions. Cavdaroglu et al. [49] developed a mixed-integer programming (MIP) model to study the restoration decision problem of interdependent power and telecommunications systems. This research only takes into account the damage to the power system. Gonzalez et al. [50] formulated an MIP model for the restoration decision problem of post-earthquake ICISs, considering four categories of interdependencies. Almoghathawi et al. [51] proposed a resilience-driven restoration model for interdependent power and water systems with the consideration of physical

dependence. Their work involves three types of disruptions: random, malevolent, and spatial failures. Sharma et al. [52] formulated a rigorous recovery optimization model to maximize the resilience of interdependent electric power and water systems against earthquakes. This model incorporates multiple recovery activities (i.e., fault detection, repair, and commissioning) and the precedence of these activities. Moreover, some researchers developed mathematical models to investigate the effects of various factors on the restoration decision problem of ICISs, such as forms of cooperation [53] and institutions and regulation [54]. As the routes of repair crews highly rely on the availability of the transportation system during the restoration process, some researchers further studied the integrated routing decision problem and restoration problem of ICIS [55,56].

Similarly, various uncertainties exist in the restoration decision problem of ICISs, and some researchers made allowance for them and established corresponding mathematical models. Zou & Chen [57] developed a stochastic optimization model to study the resilience of interdependent transportation and electric power systems, considering uncertain demands and costs of repair actions. However, this model does not specify the repair time of damaged components and the tasks of each repair crew. Alkhaleel et al. [58] built a two-stage stochastic restoration decision model of post-disaster ICIS, considering the uncertain repair time and travel time. This research utilized scenario generation and reduction methods to generate a representative set of scenarios and adopted the decomposition algorithm to solve the model over the reduced scenario set. Nevertheless, the number of scenarios is only 10, and the computational time is up to 5.8 hours in their work.

As reviewed above, most studies focused on the restoration decision problem of single CIS and multiple CISs and proposed various optimization models and solution methods. However, modeling ICISs as multigraphs and introducing a joint optimization framework under different decision-making environments has not been well studied in the literature. Some restoration decision models could not provide an executable

restoration plan for damaged ICISs [57], and the developed solution methods are less efficient for large-scale disruptions [58]. To bridge the research gap, this article studies the post-disaster restoration decision problem to enhance the resilience of ICISs under two different decision-making environments. Firstly, this article establishes a resilience-driven deterministic restoration decision model for the restoration decision problem of ICISs under certainty, in which physical interdependency is integrated for explanatory purposes. Then, under uncertainty, a two-stage stochastic model is formulated for the restoration decision problem. The repair time of damaged components is assumed to be random and represented by a set of scenarios. Next, a heuristic method derived from the greedy algorithm is developed to solve these two restoration decision models. This method produces the repair decision of each ICIS through an iterative process and is appropriate for the restoration decision problem under large-scale disruptions. Finally, numerical experiments are conducted on a series of disruptive events to investigate the value of integrating the interdependencies across systems into the restoration decision problem and exemplify the validity of the proposed method to different decision-making environments and large-scale disruptions.

The main contributions of this work are as follows: (1) developing restoration decision models of damaged ICISs under two different decision-making environments; (2) proposing a heuristic method to solve the restoration decision models; (3) exploring the significance of integrating interdependency and the performance of the proposed method. The formulated restoration decision model and the proposed solution method provide essential insights into the restoration process of ICISs and assist decision-makers in making repair plans after disasters occur. The remainder of this article is organized as follows. Section 2 describes the background of the post-disaster restoration decision problem of ICISs and gives some assumptions. Section 3 formulates the restoration decision models under two decision-making environments. Section 4 introduces a heuristic method to solve the two restoration decision models.

Section 5 presents the numerical experiments, and Section 6 provides the concluding remarks and future research avenues.

Nomenclature	
Abbreviations	
CIS	Critical infrastructure systems
ICIS	Interdependent critical infrastructure systems
MIP	Mixed-integer programming
MILP	Mixed-integer linear programming
Sets	
G^k	Network of system k
$n \in N^k$	Set of nodes in network k
$l \in L^k$	Set of lines in network k
$n \in N^{k,S}$	Set of source nodes in network k
$n \in N^{k,D}$	Set of demand nodes in network k
$n \in N^{k,A}$	Set of damaged components in network k
$l \in L_n^{1,k}$	Set of lines with the origin node being node n
$l \in L_n^{2,k}$	Set of lines with the destination node being node n
$n \in N_h^A$	Set of damaged components to be repaired at iteration h.
$n \in \widetilde{N}_h^{k,A}$	Set of unrepaired components in network k at iteration h
$s \in \Omega$	Set of repair time scenarios
Parameters	
K	Number of systems
I	Number of damaged components.
Γ	Interdependent matrix
$\bar{P}_n^{k,S}$	Maximal supply of node n in network k
$\bar{P}_n^{k,D}$	Required demand of node n in network k
$\bar{f}_l^k$	Flow capacity of line l in network k
v_n^k	The repair time of damaged component n in network k
$v_{n,s}^k$	The repair time of damaged component n in network k in scenario s
$\bar{F}$	Pre-disaster system functionality
w_k	Weight of network k
$\xi_{n \leftarrow n'}^{k \leftarrow k'}$	The minimal ratio of satisfied demand of node n' in network k' to support the operating of node n in network k
I^k	Number of damaged components in network k
ρ_s	Probability of scenario s
Q^{max}	Maximum number of components that can be repaired at each iteration
T_h'	Time interval at iteration h
M_h	Number of possible repair sequences at iteration h
X_h	A matrix that represents all possible component state vectors at iteration h
F_h	A vector that represents all possible system functionalities at iteration h
Z_h	A matrix that represents all possible repair sequences at iteration h
$\mathcal{T}_h$	A matrix that represents the time points that damaged components are repaired in matrix Z_h
$\bar{\mathcal{T}}_h$	A matrix that represents the time points that damaged components are repaired in ascending order in matrix Z_h
C_h	A matrix that represents the repaired components at each time point in $\bar{\mathcal{T}}_h$

A_h	A matrix that represents the system functionalities at each time point in $\bar{\mathcal{T}}_h$
B_h	A matrix that represents the time intervals in $\bar{\mathcal{T}}_h$
Variables	
λ_{mn}^k	Binary variable that indicates the repair sequencing decision, with 1 if task *m* in network *k* is to repair damaged component *n*, and 0 otherwise
$r_n^k(t)$	Binary variable that indicates the repair decision at time point *t*
$x_n^k(t)$	Binary variable that indicates the state of node *n* in network *k* at time point *t*
$x_l^k(t)$	Binary variable that indicates the state of line *l* in network *k* at time point *t*
$\eta^k(t)$	Binary variable that indicates the repaired network at time point *t*
$q_{n\leftarrow n'}^{k\leftarrow k'}(t)$	Binary variable that indicates the state between $n \in N^k$ and $n' \in N^{k'}$
$P_n^{k,S}(t)$	Actual supply of node n in network *k* at time point *t*
$P_n^{k,D}(t)$	Satisfied demand of node *n* in network *k* at time point *t*
$f_l^k(t)$	Actual flow on line l in network *k* at time point *t*
$\chi_{n,h}^k$	Binary variable that indicates the selected components at iteration *h*

2. Model Description and Assumptions

This section introduces the background of modeling the post-disaster restoration decision problem of ICISs and presents associated assumptions and notations.

(1) Decision-making environments

Decision-making environments refer to the information related to the restoration decision problem in this article, and there are two types of decision-making environments: certainty and uncertainty. Under certainty, decision-makers have perfect information about the restoration decision problem (i.e., the repair time of damaged components, restoration resources, and demands); the repair tasks are implemented as expected. However, the repair time, resources, and demands during the recovery process may sometimes be challenging to estimate accurately. In addition, these parameters are influenced by various factors, such as weather conditions, crew productivity, secondary disaster, and available materials. Thus, decision-makers should consider the uncertainties when disasters occur to design more appropriate repair plans. For illustration, this article considers the uncertain repair time of damaged components which is assumed to be random and represented by a set of scenarios Ω. Each scenario $s \in \Omega$ is the vector of the repair time of each damaged component, that is, $\{v_{1,s}^1, v_{2,s}^1, \dots, v_{I,s}^K\}$. In the context of a certain environment, the repair time of component *n* in network *k* is represented by v_n^k. Other uncertain factors can also be considered by

adding their realizations.

(2) Network description

This article utilizes the network-based method to model ICISs, in which nodes describe generator, transfer, and demand stations, and lines represent transmission lines, roads, and lines. Multiple interdependent systems are described as an undirected integrated network $G = \{G^k, \Gamma, k = 1, \dots, K\}$, where K denotes the number of systems, $G^k = \{N^k, L^k\}$ denotes the network of system k, and Γ represents the interconnections across systems. For each network $G^k = (N^k, L^k)$, the set of nodes and lines are denoted by N^k and L^k, respectively. Generally, there are three types of nodes: source nodes (i.e., generators), demand nodes (i.e., customers), and transshipment nodes (i.e., substations). Transshipment nodes can be regarded as demand nodes with zero demand, and then only source and demand nodes are considered. Let $N^{k,S}$ and $N^{k,D}$ denote the set of source nodes and demand nodes, respectively. Fig. 1 shows the topological network of two ICISs (i.e., K=2), in which the rectangle represents source nodes, and the circle represents demand nodes.

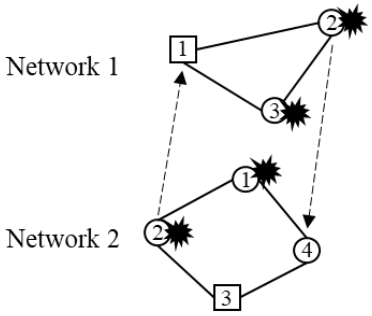

Fig. 1 The topological network of two interdependent critical infrastructure systems.

(3) System operation model

The operating mechanisms of CISs are varied and expressed by different mathematical models in the literature. Instead of modeling each type of CIS in detail, this article utilizes the general network flow model for illustration. The network flow model can describe the basic features of CISs: flows describe the movement of services or commodities (i.e., electricity, water, and gas) from source nodes (i.e., generators and plants) to demand nodes (i.e., factories and residential districts) via lines (i.e., pipes).

This model contains three types of variables: the actual supply $P_n^{k,S}$, the satisfied demand $P_n^{k,D}$, and the actual flow f_l^k. Parameters $\bar{P}_n^{k,S}$, $\bar{P}_n^{k,D}$, and $\bar{f}_l^k$ represent the maximal capacity of these variables.

(4) Interdependency modeling

There are several types of interdependencies across CISs, and this article models the physical dependency at the component-to-component level for illustration. Physical dependency describes that the state of one system (component) is determined by the output(s) of another system (component) [3]. For example, traffic lights require electricity from the substations. In the topological network of Fig. 1, the dotted line describes the interdependent relationship between these two systems. Specifically, node 2 in network 1 supports the function of node 4 in network 2, while node 2 in network 2 supports the operation of node 1 in network 1. Let binary variable $q_{n\leftarrow n'}^{k\leftarrow k'}(t)$ model this relationship:

$$q_{n\leftarrow n'}^{k\leftarrow k'}(t)=\begin{cases}0, \ if\ P_{n'}^{k',D}(t)\le \bar{P}_{k'}^{k',S}\times \xi_{n\leftarrow n'}^{k\leftarrow k'}\\ 1, \ \text{otherwise}\end{cases} \tag{1}$$

where $\xi_{n\leftarrow n'}^{k\leftarrow k'}\in[0,1]$ denote the minimal ratio of the satisfied demand of node n' in network k' to maintain the normal operating of node n in network k. Symbol "$\leftarrow$" indicates the dependency direction between these two components. Nonetheless, other types of interdependencies (i.e., cyber and geographical) can also be taken into account and modeled in this article.

(5) Damage modeling

This article studies the restoration decision problem of ICISs against natural disasters and focuses on the repair tasks of damaged components in the recovery process. The set of damaged components is known before making decisions. For illustration, this article only considers node damage, and a line's state depends on the state of its two endpoints. Also, line damage could be equivalently modeled as node damage by adding a new node in a line. Let $N^{k,A}$ denote the set of damaged components in network k. Sets $N^{1,A}$ and $N^{2,A}$ in Fig. 1 are {2, 3} and {1, 2}, and the

repair time is assumed to be {3, 4 days} and {4, 2 days}, respectively. This article assumes that the state of each component is binary, with 1 for operational and 0 otherwise. Let binary variable $x_n^k(t)$ denote the state of component *n* at time point *t*. A damaged component $n \in N^{k,A}$ is operational if it has been repaired. Moreover, if component *n* in network *k* relies on the output of component n' in network k', its state is further restricted by the binary variable $\lambda_{n \leftarrow n'}^{k \leftarrow k'}$.

(6) Recovery modeling

As the required skills to repair damaged components for different CISs are varied, the recovery activities of these networks are parallel. Meanwhile, as networks are interdependent, one network's repair plan affects another. Hence, the repair decision problem in this article entails determining a joint repair sequence Φ that can maximize the overall resilience of all networks. A joint repair sequence Φ is composed of the repair sequence φ^k of each network *k* after a disruptive event. Let binary variable λ_{mn}^k denote the repair sequencing decision, which is 1 if the *m-th* repair task in network *k* is to repair damaged component *n* and 0 otherwise. For example, the two repair sequences $\varphi^1: 2 \rightarrow 3$ and $\varphi^2: 2 \rightarrow 1$ for the case in Fig. 1 can be described by equations (2) and (3).

$$\boldsymbol{\lambda}^1 = \begin{bmatrix} \lambda_{12}^1 & \lambda_{13}^1 \\ \lambda_{22}^1 & \lambda_{23}^1 \end{bmatrix} = \begin{bmatrix} 1 & 0 \\ 0 & 1 \end{bmatrix} \tag{2}$$

$$\boldsymbol{\lambda}^2 = \begin{bmatrix} \lambda_{12}^2 & \lambda_{13}^1 \\ \lambda_{22}^1 & \lambda_{23}^1 \end{bmatrix} = \begin{bmatrix} 0 & 1 \\ 1 & 0 \end{bmatrix} \tag{3}$$

Based on the joint repair sequence $\Phi = \{\varphi^1, \varphi^2\}$ and the repair time of these damaged components, Fig. 2 illustrates the recovery process for the two ICISs. The repair tasks of these four damaged nodes are completed on the 3rd, 7th, 2nd, and 6th day. In the repair process, this article assumes that each repair crew will immediately start the next task after completing the current task. This hypothesis means ignoring the travel time between two consecutive tasks. Additionally, each repair crew can only perform one task at a time.

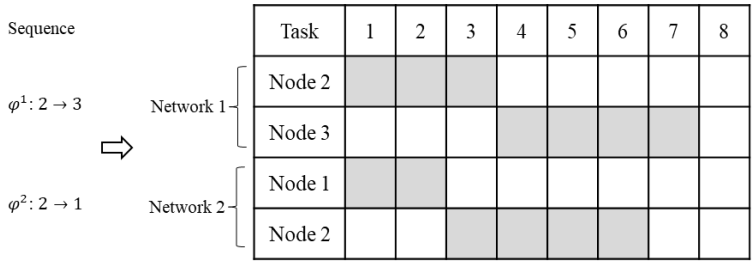

Fig. 2 The recovery process of the two interdependent networks under the joint repair sequence.

(7) Resilience metric

In the literature, researchers have proposed a variety of metrics to quantify the resilience of CISs, including magnitude-based, duration-based, integral-based, rate-based, and threshold-based metrics [59]. There is no consensus on a unified resilience metric. The adopted metrics are related to the desired attributes of concern. Sharma et al. [60] developed several resilience metrics, which could capture the characteristics of the recovery curve, but their calculations are complex. This article utilizes the "resilience loss ($\mathcal{RL}$)" to appraise the resilience of the ICISs. Here, $\mathcal{RL}$ is measured by the integral difference between the target and actual functionality curves. Note that the smaller the value of $\mathcal{RL}$, the higher the network's resilience. Considering that the top priority of CISs after a disruption is to satisfy the demands of all consumers, this article utilizes the sum of satisfied demands to quantify the system functionality of each single CIS. Then, the functionality of the ICISs is described by the weighted value for all system functionalities. Fig. 3 illustrates the restoration curve of the ICISs for the case in Fig. 1 based on the given joint repair sequence, and the shaped area represents the value of the resilience loss.

Hence, for a given joint repair sequence Φ, this resilience metric is described by Equation (4):

$$\mathcal{RL} = \int_{t_0}^{t_I} F(t)dt = \sum_{i=0}^{I-1}(\bar{F} - F(t_i)) \times (t_{i+1} - t_i) \quad (4)$$

where I is the number of damaged components, $\bar{F}$ denotes the pre-disaster system functionality, and t_i expresses the i-th time point. At each time point t_i $(i \geq 1)$, only one damaged component from all networks is repaired, and the weighted system functionality $F(t_i)$ of ICIS is changed and calculated by Equation (5).

$$F(t_i) = \frac{1}{K}\sum_{k=1}^{K} w_k \sum_{n \in N^{k,D}} P_n^{k,D}(t_i) \quad (5)$$

where K is the number of systems of concern, w_k represents the weight of network k, and $P_n^{k,D}(t_i)$ denotes the satisfied demand of node n in network k at t_i. For normalization, this article utilizes the reciprocal of the aggregate demand as the weight of each system, i.e., $w_k = 1/\sum_{n \in V^{k,D}} \bar{P}_n^{k,D}$, and then the upper value of $F(t_i)$ is 1.

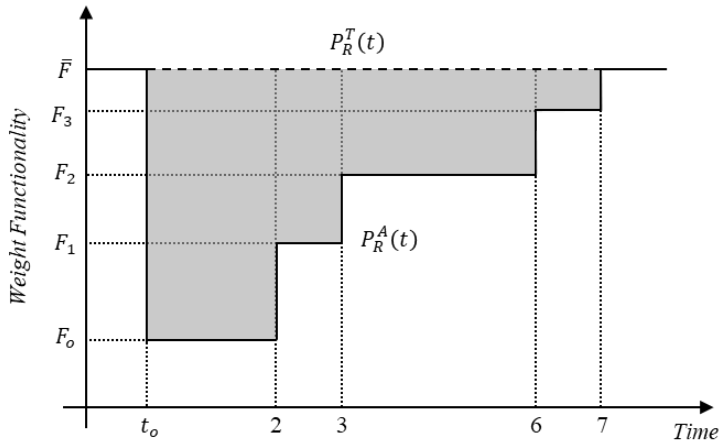

Fig. 3 The restoration curve of the interdependent critical infrastructure systems based on the given joint repair sequence.

In the decision-making environment under uncertainty, the resilience loss under scenario s is represented by $\mathcal{RL}_s$ and calculated based on the joint repair sequence Φ. Then, the expected resilience losses $\overline{\mathcal{RL}}$ is taken as the metric to evaluate the performance of the combined repair sequence. Nonetheless, other properties (e.g., total cost and completion time) of the repair sequence decision can also be involved in the restoration decision problem by adding related constraints.

(8) Model assumptions

Based on the above model description, the assumptions of this article are summarized as follows:

- This article models multiple ICISs as an undirected integrated network and considers the bidirectional physical dependencies among systems.
- Transshipment nodes are regarded as demand nodes with zero demand.
- A general network flow model is adopted to mimic the operating mechanisms of CISs, and the total satisfied demand is utilized to measure system functionality.

- Only node damage is considered, while line damage could be modeled as node damage by adding a new node in a line.
- The uncertain repair time of damaged components is considered and represented by a set of scenarios Ω.
- At each time point, only one damaged component is repaired in all networks.
- The recovery activities of interdependent networks are parallel, and the repair sequence of each network *k* forms a joint repair sequence.

3. Mathematical Formulation

This section introduces the resilience-driven restoration decision models of post-disaster ICISs in the decision-making environment under certainty and uncertainty. For a disruptive event with *I* damaged components of *K* interdependent systems, the restoration decision problem is to search for a joint repair sequence Φ with the minimum resilience loss $\mathcal{RL}$. Mathematically, this problem is formulated as a two-stage optimization model. The first stage seeks a joint repair sequence Φ considering its future effect, and the effect here is evaluated by the resilience loss in the second stage for all possible scenarios. The general formulation of this restoration decision model is described as follows:

$$\min_{\boldsymbol{\lambda}} E_{\xi}\left[\mathcal{Q}\left(\boldsymbol{\lambda}, \xi(s)\right)\right]$$

$$s.t.\ \ \boldsymbol{A\lambda} = \boldsymbol{b}, \boldsymbol{\lambda} \in \boldsymbol{\Lambda} \tag{6}$$

where $\boldsymbol{\lambda} \in \boldsymbol{\Lambda}$ is the first-stage decision variable vector and $\mathcal{Q}\left(\boldsymbol{\lambda}, \xi(s)\right)$ is the optimal value of the second-stage problem.

$$\mathcal{Q}\left(\boldsymbol{\lambda}, \xi(s)\right) = \begin{Bmatrix} \min\limits_{\boldsymbol{y}(s)} g(s)^T \boldsymbol{y}(s) \\ \boldsymbol{T}(s)\boldsymbol{\lambda} + \boldsymbol{W}(s)\boldsymbol{y}(s) = \boldsymbol{h}(\boldsymbol{s}) \\ \boldsymbol{y}(s) \in \mathbb{Y} \end{Bmatrix}, \forall s \in \Omega \tag{7}$$

where $\boldsymbol{y}(s) \in \mathbb{Y}$ is the second-stage decision variable vector, including $r_n^k\left(t_{i,s}\right)$, $x_n^k\left(t_{i,s}\right)$, $x_l^k\left(t_{i,s}\right)$, $\eta^k\left(t_{i,s}\right)$, $q_{n\leftarrow n'}^{k\leftarrow k'}\left(t_{i,s}\right)$, $P_n^{k,D}\left(t_{i,s}\right)$, $P_n^{k,S}\left(t_{i,s}\right)$, and $f_l^k\left(t_{i,s}\right)$. Set Ω denotes the set of possible scenarios. The objective function $g(s)^T\boldsymbol{y}(s)$ represents the

resilience loss $\mathcal{RL}_s$ of scenario $s \in \Omega$ and is calculated by Equation (4). Note that the number of scenarios in Ω is 1 in the decision-making environment under certainty.

Based on the description of the first-stage decision variable λ_{mn}^k in Section 2, Constraints (8)-(10) are the related constraints in Equation (6).

$$\sum_{m=1}^{I^k} \lambda_{mn}^k = 1, \forall n \in N^{k,A}, k \tag{8}$$

$$\sum_{n \in N^{k,A}} \lambda_{mn}^k = 1, \forall m, k \tag{9}$$

$$\lambda_{mn}^k \in \{0,1\}, \forall m, n, k \tag{10}$$

Constraint (8) ensures that each damaged component in network k should be repaired, in which I^k denotes the number of damaged components in network k. Constraint (9) guarantees that each task is assigned one damaged component. Constraint (10) enforces variable λ_{mn}^k as binary. The following will introduce the mathematical models in decision-making environments under certainty and uncertainty, respectively.

3.1 Decision-making under certainty

There is only one repair time scenario in the decision-making environment under certainty. Hence, the mathematical model is described as follows:

$$\min_{\boldsymbol{\lambda}} \min_{\boldsymbol{y}} q^T \boldsymbol{y} = \min_{\boldsymbol{\lambda}, \boldsymbol{y}} \mathcal{RL}(\boldsymbol{\lambda}, \boldsymbol{y}) = \sum_{i=0}^{I-1} (\bar{F} - F(t_i))(t_{i+1} - t_i)$$

$$s.t. \ \boldsymbol{A\lambda} = \boldsymbol{b}, \boldsymbol{\lambda} \in \boldsymbol{\Lambda}$$

$$\boldsymbol{T\lambda} + \boldsymbol{W\boldsymbol{y}} = \boldsymbol{h}$$

$$\boldsymbol{y} \in \mathbb{Y} \tag{11}$$

The constraints related to the second-stage decision variable $\boldsymbol{y}$ are grouped into four categories: constraints of the network flow model, repair decisions, component states, and interdependency.

(1) Constraints of network flow model

Constraints (12)-(16) are the constraints of network flow model. Constraints (12) and (13) guarantee the nodal balance for each system's supply node and demand node, respectively. Here, $L_n^{1,k}$ and $L_n^{2,k}$ denote the set of lines with the origin and destination

node being node n, respectively. Constraint (14) enforces the flow on each line to be less than its maximal capacity. Constraints (15) and (16) limit the capacity of source and demand nodes, respectively.

$$P_n^{k,S}(t_i) - \sum_{l\in L_n^{1,k}} f_l^k(t_i) + \sum_{l\in L_n^{2,k}} f_l^k(t_i) = 0, \forall n \in N^S, \forall i, k \quad (12)$$

$$P_n^{k,D}(t_i) + \sum_{l\in L_n^{1,k}} f_l^k(t_i) - \sum_{l\in L_n^{2,k}} f_l^k(t_i) = 0, \forall n \in N^D, \forall i, k \quad (13)$$

$$-\bar{f}_l^k x_l^k(t_i) \le f_l^k(t_i) \le \bar{f}_l^k x_l^k(t_i), \forall l \in L, \forall l \in L, i, k \quad (14)$$

$$0 \le P_n^{k,S}(t_i) \le \bar{P}_n^{k,S} x_n^k(t_i), \forall n \in N^{k,S}, i, k \quad (15)$$

$$0 \le P_n^{k,D}(t_i) \le \bar{P}_n^{k,D} x_n^k(t_i), \forall n \in N^{k,D}, i, k \quad (16)$$

(2) Constraints of repair decisions

The repair decision $r_n^k(t)$ should comply with the joint repair sequence Φ, and Constraints (17)–(25) represent the constraints of the repair decisions. Constraint (17) enforces that damaged components in each system can be repaired once at most. Constraint (18) guarantees the repair sequence of each network is parallel, indicating that the repair sequence of network k only contains the damaged component in this network. Constraint (19) describes the binary variable $\eta^k(t_i)$, with 1 if one damaged component in network k is repaired at the time point t_i and 0 otherwise. Constraint (20) ensures one damaged component must be repaired at each time point t_i when $i \ge 1$, while Constraint (21) enforces that no components are repaired at the initial time point t_0. Constraint (22) expresses the calculation of time point t_i. Constraint (23) ensures the non-decreasing time points from t_0 to t_I. Constraint (24) describes the completion time of each damaged component according to the joint repair decision λ_{mn}^k. Constraint (25) enforces variables $r_n^k(t_i)$ and $\eta_i^k(t_i)$ as binary.

$$\sum_{i=0}^{I} r_n^k(t_i) \le 1, \forall n \in N^{k,A}, k \quad (17)$$

$$r_n^k(t_i) = 0, n \notin N^{k,A}, k \quad (18)$$

$$\eta^k(t_i) = \sum_{n\in N^{k,A}} r_n^k(t_i), \forall i, k \quad (19)$$

$$\sum_{k=1}^{K} \eta^k(t_i) = 1, \forall i \ge 1 \quad (20)$$

$$\sum_{k=1}^{K} \eta^k(t_i) = 0, i = 0 \quad (21)$$

$$t_i = \sum_{k=1}^{K} \eta^k(t_i)\left(\sum_{n\in N^{k,A}} \sum_{i'=0}^{i} r_n^k(t_{i'}) v_n^k\right), \forall i \tag{22}$$

$$t_{i+1} - t_i \geq 0, \forall i \tag{23}$$

$$\sum_{n'=1}^{n} \sum_{m=1}^{I^k} \lambda_{mn'}^k v_{n'}^k = \sum_{i=0}^{I} r_n^k(t_i)\, t_i, \forall k, n \in N^{k,A} \tag{24}$$

$$r_n^k(t_i), \eta_i^k(t_i) \in \{0,1\}, \forall i, n, k \tag{25}$$

(3) Constraints of component states

Constraints (26)–(29) are the constraints of component states. Constraint (26) represents the relationship between the state of damaged components and the repair decision. Constraint (27) states that all undamaged components are normal. Constraint (28) describes that line *l's* state depends on its endpoints' states. Constraint (29) enforces binary decisions.

$$x_n^k(t_i) \leq \sum_{i'=0}^{i} r_n^k(t_i), \forall n \in N^{k,A}, i, k \tag{26}$$

$$x_n^k(t_i) \leq 1, \forall n \in N^k \backslash N^{k,A}, i, k \tag{27}$$

$$x_l^k(t_i) = x_{o(l)}^k(t_i) x_{d(l)}^k(t_i), \forall l \in L, i, k \tag{28}$$

$$x_n^k(t_i), x_l^k(t_i) \in \{0,1\}, \forall n \in N^k, i, k \tag{29}$$

(4) Constraints of interdependency

Constraints (30)–(32) describe the limitations of physical interdependency. Constraint (30) states that the binary variable $\lambda_{n\leftarrow n'}^{k\leftarrow k'}(t_i)$ is 0 if the real satisfied demand $P_{n'}^{k'}(t_i)$ of node n' is less $\xi_{n\leftarrow n'}^{k\leftarrow k'} \times \bar{P}_{n'}^{k'}$. Constraint (31) describes the state of component *n* depends on the state of its interdependent relationship. Constraint (32) enforces binary decisions.

$$\lambda_{n\leftarrow n'}^{k\leftarrow k'}(t_i) \leq \frac{P_{n'}^{k'}(t_i)}{\xi_{n\leftarrow n'}^{k\leftarrow k'} \times \bar{P}_{n'}^{k'}}, \forall \{n, n'\} \in \Gamma, i \tag{30}$$

$$x_n^k(t_i) \leq \lambda_{n\leftarrow n'}^{k\leftarrow k'}(t_i), \forall \{n, n'\} \in \Gamma, i \tag{31}$$

$$\lambda_{n\leftarrow n'}^{k\leftarrow k'} \in \{0,1\}, \forall \{n, n'\} \in \Gamma, i \tag{32}$$

Due to the product terms in Equation (11) and Constraint (22), this optimization model is nonlinear and can be transformed into a mixed-integer linear programming

(MILP) model by using the McCormick method [61]. Three new variables $\theta_n^k(t_i)$, $\alpha_n^k(t_i)$, and $\beta_n^k(t_i)$ are introduced, and their expressions are:

$$\theta_n^k(t_i) = \eta^k(t_i) \times \sum_{i'=0}^{i} r_n^k(t_{i'}) \tag{33}$$

$$\alpha_n^k(t_i) = \theta_n^k(t_{i+1}) \times F(t_i) \tag{34}$$

$$\beta_n^k(t_i) = \theta_n^k(t_i) \times F(t_i) \tag{35}$$

These three new variables are the product of a binary variable and a real-valued variable with a lower and upper bound. Then, these three new variables can be linearized by adding the following constraints.

$$0 \le \theta_n^k(t_i) \le \eta^k(t_i) \tag{36}$$

$$\eta^k(t_i) - 1 + \sum_{i'=1}^{i} r_n^k(t_{i'}) \le \theta_n^k(t_i) \le \sum_{i'=1}^{i} r_n^k(t_{i'}) \tag{37}$$

$$0 \le \alpha_n^k(t_i) \le F(t_i) \tag{38}$$

$$F(t_i) - \left(1 - \theta_n^k(t_{i+1})\right)\mathbb{M} \le \alpha_n^k(t_i) \le \theta_n^k(t_{i+1}) \times \mathbb{M} \tag{39}$$

$$0 \le \beta_n^k(t_i) \le F(t_i) \tag{40}$$

$$F(t_i) - \left(1 - \theta_n^k(t_i)\right) \times \mathbb{M} \le \beta_n^k(t_i) \le \theta_n^k(t_i) \times \mathbb{M} \tag{41}$$

where parameter $\mathbb{M}$ in Constraints (39) and (41) denotes the upper bound of $F(t_i)$ and is determined by $\sum_{k=1}^{K} w_k \sum_{n \in N^{k,D}} \bar{P}_n^{k,D}$.

Finally, Equation (42) describes the objective function in Equation (11), and Equation (43) represents the linearization of Constraint (22).

$$\min_{\boldsymbol{\lambda},\boldsymbol{y}} \mathcal{RL}(\boldsymbol{\lambda},\boldsymbol{y}) = \sum_{i=0}^{I-1}\left[\bar{F}(t_{i+1} - t_i) - \sum_{k=1}^{K}\sum_{n \in N^{k,A}}\left(\alpha_n^k(t_i) - \beta_n^k(t_i)\right)v_n^k\right] \tag{42}$$

$$t_i = \sum_{k=1}^{K}\sum_{n \in N^{k,A}} \theta_n^k(t_i) v_n^k, \forall i \tag{43}$$

3.2 Decision-making under uncertainty

In the decision-making environment under uncertainty, this article considers the uncertain repair time of damaged components. Stochastic optimization has been widely adopted to model decision-making under uncertainty, in which some parameters are uncertain but follow known probability distributions [62]. This article also utilizes this approach to study the restoration decision models of post-disaster ICISs in the decision-

making environment under uncertainty. The repair time of each damaged component is assumed to follow a known distribution function. Then, a scenario set Ω is generated to represent the uncertainty through scenario generation methods (i.e., random sampling or Latin hypercube sampling). Thus, the original two-stage stochastic optimization model is transferred into a deterministic optimization model which aims to determine a joint repair sequence Φ with the minimal expected resilience loss $\overline{\mathcal{RL}}$ over the scenario set Ω:

$$\min_{\boldsymbol{\lambda}} E_{\xi}\left[\mathcal{Q}\left(\boldsymbol{\lambda}, \xi(s)\right)\right] = \min_{\boldsymbol{\lambda}} \sum_{s\in\Omega} \rho_s \min_{\boldsymbol{y(s)}} \mathcal{RL}\left(\boldsymbol{\lambda}, \boldsymbol{y(s)}\right)$$

$$= \min_{\boldsymbol{\lambda}, \boldsymbol{y(s)}} \sum_{s\in\Omega} \rho_s \sum_{i=0}^{I-1} \left(\bar{F} - F(t_{i,s})\right)\left(t_{(i+1),s} - t_{i,s}\right)$$

$$s.t.\ \ \boldsymbol{A\lambda} = \boldsymbol{b}, \boldsymbol{\lambda} \in \boldsymbol{\Lambda}$$

$$\boldsymbol{T\lambda} + \boldsymbol{W(s)y(s)} = \boldsymbol{h(s)}\ , \forall s \in \Omega$$

$$\boldsymbol{y(s)} \in \mathbb{Y}, \forall s \in \Omega \tag{44}$$

where ρ_s denotes the probability of scenario *s*, $t_{i,s}$ denotes the *i*-th time point under scenario *s*, and $F(t_{i,s})$ denotes the weighted system functionality of ICISs at $t_{i,s}$ under scenario *s*. The objective function of this model is to minimize the expected value of the resilience loss of each scenario $s \in \Omega$ under the joint repair decision $\boldsymbol{\lambda}$**.** This model subjects to the constraints of the first stage (i.e., Constraints (8)-(10)) and the constraints of the second stage for each $s \in \Omega$ (i.e., Constraints (12)-(32) for each $s \in \Omega$). This model could also be linearized using the McCormick method [61].

4. Solution Algorithm

This section introduces a heuristic method to solve the restoration decision models of disrupted ICISs under two decision-making environments. Both can be transferred into an MILP model and directly solved by optimization software under small-scale disruptions. The restoration decision problems are NP-hard, so the direct solution method may fail under large-scale disturbances. To this end, this article draws on the greedy algorithm and proposes a heuristic method to tackle this issue. This method

comprises a selection principle and a matrix-based approach and seeks the joint repair sequence of damaged ICISs via an iterative process. At each iteration, the selection principle determines a set with a limited number of damaged components, while the matrix-based approach determines the optimum repair sequence.

4.1 A selection principle

This section will introduce a selection principle to select a set of damaged components (N_h^A) to be repaired at iteration h. The number of selected components is limited as the matrix-based approach cannot handle large-scale disruptions. Also, fixing the selected components could benefit the interdependent systems the most. Let parameter Q^{max} denote the maximum number of components that can be repaired at each iteration. The benefit of fixing the components in N_h^A is measured by the ratio of the system functionality to the minimum required time. Then, this problem can be modeled as follows:

$$\max_{N_h^A \in \tilde{N}^A} \rho = \frac{F(N_h^A)}{\min T(N_h^A)} \tag{45}$$

$$0 < crad(N_h^A) \leq Q^{max} \tag{46}$$

where N_h^A indicates the set of damaged components that are selected at iteration h, $F(N_h^A)$ denotes the integrated system functionality of ICISs after the damaged components in N_h^A are repaired, and $crad(N_h^A)$ expresses the number of components in N_h^A. When there are multiple repair crews in a single system, the completion time for repairing the damaged components depends on the schedule of the repair crews. As shown in Fig. 4, there are four damaged components $\{c_1, c_2, c_3, c_4\}$ and two repair crews in a single system. The required repair time for the damaged components is 1, 1.5, 1, and 2 days, respectively. Schedules 1 and 2 are the two feasible schedules to repair those four components, and their completion time is 3 and 3.5 days. In this context, let $\min T(N_h^A)$ represent the minimal completion time for repairing the damaged components in N_h^A, and this value is 3 days for the case in Fig. 4.

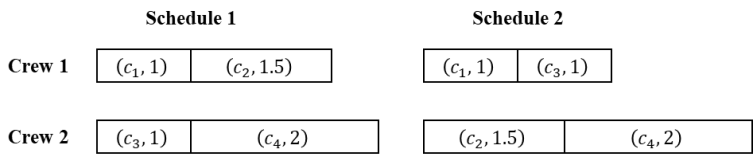

Fig. 4 An illustration for two different schedules.

Step 1: Determine a feasible time interval

Suppose that damaged components are allocated to repair crews according to their required time and components with less repair time are prioritized for repair. Then, a series of time points can be obtained when damaged components are repaired. Sort these time points in ascending order, and let $T_h^{Q^{max}+1}$ denote the $(Q^{max}+1)$-*th* time point at iteration *h*. Then, under time interval $T_h' = T_h^{Q^{max}+1} - \varepsilon$ (ε is a tiny positive number), the maximal number of damaged components that can be repaired will not be larger than Q^{max}. For the case in Fig. 4, when there is only one repair crew, the sorted time points are 1, 2, 3.5, and 5.5 days. If setting the interval to 3.4 days (less than 3.5 days), a maximum of two components can be repaired.

Step 2: Find an optimum set

To select an optimum set under the time constraint, an MILP model is developed and described by Equation (47) and Constraints (48) – (51). Equation (47) denotes the objective function of this model. Constraint (48) represents the constraints of system operation model. Constraint (49) expresses the time constraint. Here, parameter $\widetilde{N}_h^{k,A}$ expresses the set of unrepaired components in network *k* at iteration *h*, and $\chi_{n,h}^k$ denotes the binary decision variable, with 1 if component $n \in \widetilde{N}^{k,A}$ is selected at iteration *h*, and 0 otherwise. Constraint (50) ensures that the state of damaged component $n \in \widetilde{N}_h^{k,A}$ will be operational once this component is selected. Constraint (51) represents the nature of decision variables.

$$\max_{\{\boldsymbol{P},\boldsymbol{f},\boldsymbol{\chi}\}} \boldsymbol{F} = \sum_{k=1}^{K} w_k \times \sum_{n \in N^{k,D}} P_n^{k,D} \tag{47}$$

$$\text{Constraints (11) – (15)} \tag{48}$$

$$\sum_{n \in \widetilde{N}^{k,A}} \chi_{n,h}^k \times v_n^k \leq T_h' \tag{49}$$

$$x_n^k \leq \chi_{n,h}^k, \forall n, k \tag{50}$$

$$\chi_{n,h}^k, x_n^k \in \{0,1\}, \forall n, k \tag{51}$$

This selection principle can be modified to solve the stochastic restoration decision model: replacing the repair time with the expected values in Steps 1 and 2, then determining the set of repaired components at each iteration.

4.2 A matrix-based approach

A matrix-based approach utilizes matrix operations to determine the optimum joint repair sequence of the damaged components in N_h^A. Let I_h denotes the number of damaged components in N_h^A, and then the maximum number of possible repair sequences is $I_h!$. To calculate their resilience losses, the number of required system functionalities is $I_h \times I_h!$ (more than 36 million with $I_h = 10$). But in fact, the number of all possible system functionalities is only 2^{I_h} (1024 with $I_h = 10$) because each component has only two states: operational or damaged. Thus, we first compute and store all possible system functionalities in a matrix, then calculate each repair sequence's resilience loss by calling this matrix. This processing method highly reduces the computational burden. The matrix-based approach can be realized as follows:

Step 1: Calculate system functionality

List all possible component states in N_h^A and calculate the system functionality for each component state vector, as shown in Equation (52). Here, X_h represents a $2^{I_h} \times I_h$-matrix, F_h denotes a $2^{I_h} \times 1$-vector. Each row in Equation (52) expresses a component state vector and the corresponding system functionality. Note that the state of components not in N_h^A is either 1 or 0, with 1 indicating that the component is repaired or not damaged and 0 otherwise.

$$[X_h \ F_h] = \begin{bmatrix} 0 & 0 & \ldots & 0 & \cdots & 0 & 0 & \ldots & 0 & F_1 \\ 0 & 0 & \cdots & 0 & \cdots & 0 & 0 & \cdots & 1 & F_2 \\ \ldots & & \cdots & & \ldots & & \ldots & & \ldots & \cdots \\ 1 & 1 & \cdots & 1 & \cdots & 1 & 1 & \cdots & 1 & F_{2^{Ih}} \end{bmatrix} \tag{52}$$

Step 2: List repair sequence matrix

We first re-number the damaged components in N_h^A from 1 to I_h, and then list all possible repair sequences in an $M_h \times I_h$-matrix Z_h, as shown in Equation (53). Here, M_h represents the number of possible repair sequences, and its value is $\prod_{k=1}^{K}(I_h^k!)$,

and I_h^k denotes the number of damaged components in network k at iteration h. Each row represents a repair sequence, and the numeral indicates the repair order of the component.

$$Z_h = \begin{bmatrix} 1 & 2 & \dots & I_h - 1 & I_h \\ 1 & 2 & \dots & I_h & I_h - 1 \\ \dots & \dots & \dots & \dots & \dots \\ I_h & I_h - 1 & \dots & 2 & 1 \end{bmatrix} \tag{53}$$

Step 3: Calculate the time point matrix

According to matrix Z and the repair time $\{v_n^k\}$ of damaged components in N_h^A, we can determine the time points that damaged components are repaired. These time points are described by an $M_h \times I_h$-matrix $\mathcal{T}_h$ in Equation (54):

$$\mathcal{T}_h = \begin{bmatrix} \tau_{11} & \tau_{12} & \dots & \tau_{1(I_h-1)} & \tau_{1I_h} \\ \tau_{21} & \tau_{22} & \dots & \tau_{2I_h} & \tau_{1(I_h-1)} \\ \dots & \dots & \dots & \dots & \dots \\ \tau_{MI_h} & \tau_{M(I_h-1)} & \dots & \tau_{M2} & \tau_{M1} \end{bmatrix} \tag{54}$$

Sorting matrix $\mathcal{T}_h$ in terms of the time points in ascending order, we can obtain the time points from t_{h1} to t_{hI_h} for each repair sequence in the matrix Z_h. These time points are described by an $M_h \times I_h$-matrix $\bar{\mathcal{T}}_h$ in Equation (55). Also, the component that is repaired at each time point is determined and expressed by an $M_h \times I_h$-matrix C_h in Equation (56). Here, $\bar{\tau}_{ab}$ denotes the *b-th* time point of the *a-th* repair sequence, and C_{ab} denotes the component is repaired at the time point $\bar{\tau}_{ab}$.

$$\bar{\mathcal{T}}_h = \begin{bmatrix} \bar{\tau}_{11} & \bar{\tau}_{12} & \dots & \bar{\tau}_{1(I_h-1)} & \bar{\tau}_{1I_h} \\ \bar{\tau}_{21} & \bar{\tau}_{22} & \dots & \bar{\tau}_{2(I_h-1)} & \bar{\tau}_{2I_h} \\ & & \dots & & \dots \\ \bar{\tau}_{M1} & \bar{\tau}_{M2} & \dots & \bar{\tau}_{M(I_h-1)} & \bar{\tau}_{MI_h} \end{bmatrix} \tag{54}$$

$$C_h = \begin{bmatrix} C_{11} & C_{12} & \dots & C_{1(I_h-1)} & C_{1I_h} \\ C_{21} & C_{22} & \dots & C_{2(I_h-1)} & C_{2I_h} \\ & & \dots & & \dots \\ C_{M1} & C_{M2} & \dots & C_{M(I_h-1)} & C_{MI_h} \end{bmatrix} \tag{55}$$

Step 4: Calculate resilience loss

We first obtain the state of each component at each time point according to matrix C_h and then calculate the system functionality at each time point by calling matrix F_h. Matrix A_h in Equation (57) represents the system functionalities from time point t_{h0} to $t_{h(I_h-1)}$ for each repair sequence in matrix Z_h. Matrix B_h in Equation (58)

denotes the time intervals for each repair sequence in matrix Z_h.

$$A_h = \begin{bmatrix} \bar{F}_{10} & \bar{F}_{11} & \cdots & \bar{F}_{1(I_h-2)} & \bar{F}_{1(I_h-1)} \\ \bar{F}_{20} & \bar{F}_{21} & \cdots & \bar{F}_{2(I_h-2)} & \bar{F}_{2(I_h-1)} \\ & & \cdots & & \cdots \\ \bar{F}_{M0} & \bar{F}_{M1} & \cdots & \bar{F}_{M(I_h-2)} & \bar{F}_{M(I_h-1)} \end{bmatrix} \tag{56}$$

$$B_h = \begin{bmatrix} \bar{\tau}_{11} & \bar{\tau}_{12} - \bar{\tau}_{11} & \cdots & \bar{\tau}_{1(I_h-1)} - \bar{\tau}_{1(I_h-2)} & \bar{\tau}_{1I_h} - \bar{\tau}_{1(I_h-1)} \\ \bar{\tau}_{21} & \bar{\tau}_{22} - \bar{\tau}_{21} & \cdots & \bar{\tau}_{2(I_h-1)} - \bar{\tau}_{2(I_h-2)} & \bar{\tau}_{2I_h} - \bar{\tau}_{2(I_h-1)} \\ & & \cdots & & \cdots \\ \bar{\tau}_{M1} & \bar{\tau}_{M2} - \bar{\tau}_{M1} & \cdots & \bar{\tau}_{M(I_h-1)} - \bar{\tau}_{M(I_h-2)} & \bar{\tau}_{MI_h} - \bar{\tau}_{M(I_h-1)} \end{bmatrix} \tag{57}$$

Then, the resilience loss vector RL_h of all repair sequences in matrix Z_h can be determined by the following Equation (59):

$$RL_h = (A_h \circ B_h)d_h \tag{58}$$

where symbol "$\circ$" denotes the Hadamard product and d_h is an $M_h \times 1$ vector with each element as one. Then, the optimum repair sequence in matrix Z_h with the minimum value in RL_h is determined.

For the stochastic restoration decision model of ICISs, we utilize this matrix-based approach to calculate the resilience loss vector $RL_{h,s}$ under each scenario $s \in \Omega$. The expected resilience loss vector ($\overline{RL_h}$) for all repair sequences is determined by the expected value of each $RL_{h,s}$:

$$\overline{RL_h} = \sum_{s\in\Omega} \rho_s RL_{h,s} = \sum_{s\in\Omega} \rho_s \left(A_{h,s} \circ B_{h,s}\right) d_h \tag{59}$$

5. Numerical Analysis

This section first illustrates the restoration decision model and investigates the value of interdependency on two small-scale ICISs. Then, the proposed method is applied to two larger-scale ICISs under a variety of disruptive events to demonstrate its efficiency. The experiments are performed on a desktop computer with Intel i7-10700 eight-core @ 2.90 GHz and 16 GB memory, and MATLAB solves the optimization model with CPLEX Toolbox.

5.1 The value of integrating interdependency

A typical case study is presented on two small-scale ICISs to illustrate the

formulated restoration decision model and the value of integrating interdependency into the restoration decision problem of damaged ICISs. Fig. 5 shows the layouts of these two systems, including the IEEE 14 bus power system and the adapted gas system with 16 nodes. The rectangle denotes source nodes; the circle indicates demand nodes; and the dotted line with an arrow represents the interdependent relationship between these two systems. For example, dotted line 3-13 indicates the production of node 13 in the gas system depends on the state of node 3 in the power system. A disruptive event caused 10 components to be damaged, including nodes 2, 7, 9, 10, and 14 in the power system and nodes 4, 9, 10, 13, and 15 in the gas system. This section assumes that the required time to repair these 10 components is in the range of 5 to 10 days. Then, we randomly generate one repair time scenario for the deterministic restoration model and 1000 scenarios for the stochastic restoration model.

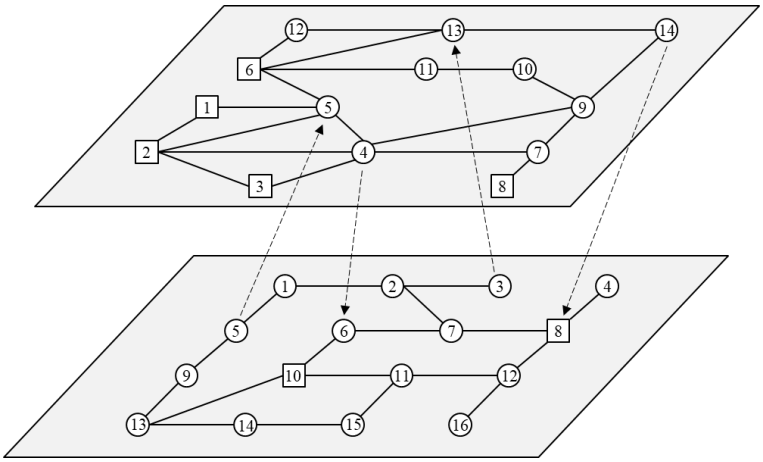

Fig. 5 The layout of an interdependent power-gas system.

This article considers two repair decision patterns to illustrate the value of integrating interdependency in the restoration decision problem: joint and separate. The joint pattern takes these two systems as a whole and seeks an integrated repair plan to minimize their resilience losses simultaneously. The separate pattern neglects the interdependent relationship and independently determines the optimal repair plan for each system. Then, we evaluate the real resilience loss under this decision pattern according to their repair plans. Table 1 shows the repair plans and resilience losses for

the disruptive event under these two repair decision patterns and decision-making environments, respectively. In the decision-making environment under certainty, the repair plans are the same for the gas system; the damaged node 14 in the power system has the highest priority to be repaired under the joint decision pattern, while this node ranks third under the separate decision pattern; the resilience losses under these two decision patterns are 9.99 and 13.61, with a difference of 36.24%; the resilience loss is reduced from 9.23 to 7.63 for the power system, and from 18.00 to 12.36 for the gas system. In the decision-making environment under uncertainty, the damaged node 14 in the power system still has the highest repair priority under the joint decision pattern; the expected resilience losses under these two patterns are 9.72 and 13.68, with a difference of 40.74%. The results also show that the repair plans for the gas system under these two decision-making environments are different (node 10 has the highest repair priority under uncertainty), which indicates that uncertainty could affect the repair decision.

Table 1

The repair plans and resilience losses of the interdependent power and gas system under two repair decision patterns and decision-making environments.

Pattern	**Decision-making under certainty**		**Decision-making under uncertainty**	
	Repair Plan	$\mathcal{RL}$	Repair Plan	$\overline{\mathcal{RL}}$
Joint	P: 14→9→2→10→7 G: 15→10→4→13→9	9.99	P: 14→9→2→10→7 G: 10→15→4→13→9	9.72
Separate	P: 9→2→14→10→7 G: 15→10→4→13→9	13.61	P: 9→2→14→10→7 G: 15→10→4→13→9	13.68

Moreover, Fig. 6 shows the restoration curve of the interdependent systems under these two repair decision patterns in the decision-making environments under certainty. Results show that the joint repair decision pattern performs better than the separate one. The reason is that node 8 in the gas system is a source node, and its operation state depends on node 14 in the damaged power system. To quickly restore the system functionality of the gas system, node 14 should have high repair priority. However, the separate repair decision pattern does not consider their interdependency.

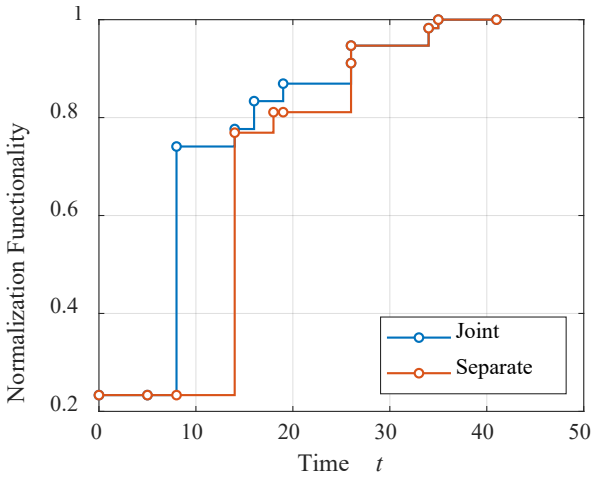

Fig. 6 Restoration curve of the interdependent systems under the joint and separate decision patterns.

For further illustration, we generate 50 disruptive events and compare the resilience loss under these two decision patterns in the decision-making environment under certainty. The number of interdependent node pairs (NNP) is set to 4, 6, and 8. Also, for each number of node pairs, 20 different interdependent matrices are randomly generated. Fig. 7 (a) and (b) show the distribution of the average and maximal differences of the resilience losses under the joint and separate decision patterns, respectively. The median values are 4.68%, 6.30%, and 7.15% for the average difference, and 35.37%, 37.49%, and 39.75% for the maximal difference, respectively. Furthermore, Fig. 8 shows the complementary cumulative distribution of the difference between the joint and separate repair decision patterns over the 1000 different scenarios (50 disruptive events × 20 interdependent matrices) with NNP = 4, 6, and 8. Results indicate that the difference will be larger with the increase in interdependency. For NNP = 4, the differences of 41.8% (17.2%) scenarios are larger than 1% (10%), while the percentages are 51.6% (22.8%) for NNP = 6 and 63.8% (29.1%) for NNP = 8. Hence, there are significant benefits for integrating interdependency into the restoration decision problem of damaged ICISs, and the value of the benefit can be up to 30% in some cases.

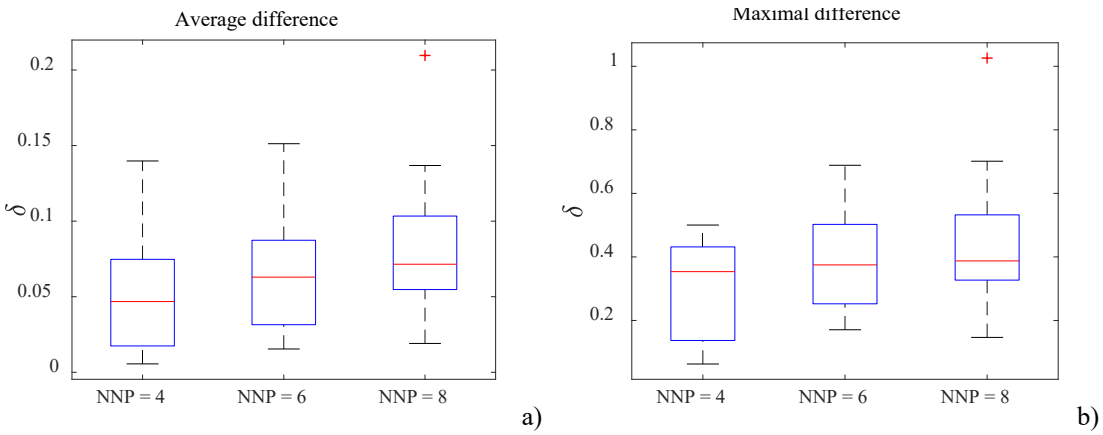

Fig. 7 The distribution of the differences in resilience losses under the joint and separate decision pattern: a) average difference; b) maximal difference.

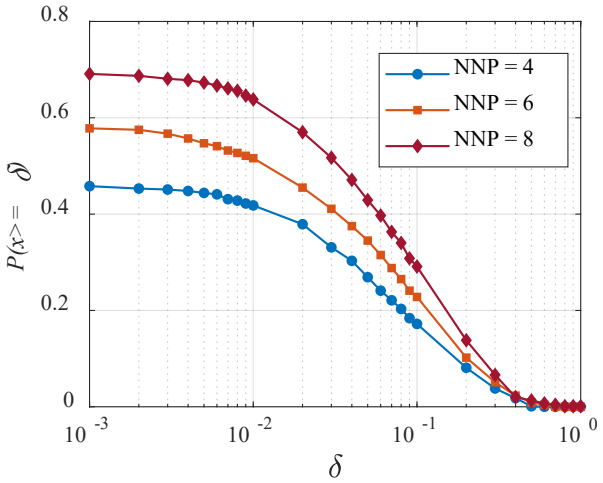

Fig. 8 The complementary cumulative distribution of the relative error between the joint and separate repair decision patterns over the 1000 different scenarios (50 disruptive events × 20 interdependent matrices) for each number of interdependent node pairs.

5.2 Performance analysis of the heuristic method

This section implements experiments to illustrate the superiority of the proposed heuristic method in the decision-making environment under certainty. The proposed method is adopted for an interdependent electric power and water supply system from Shelby County, TN, USA. Fig. 9 depicts the geographical layouts, and the number of nodes in these two systems is 81 and 64, respectively. For more detailed information, refer to Chang et al. [63]. Electric power systems need water for cooling and emission control, while the operation of water pumps requires electricity [64]. To describe their connections, we generate 15 fictitious interdependent node pairs. Also, this section considers three types of intensities to reflect the earthquake's impact on these two

systems: Intensity 1 with 20% of nodes damaged; Intensity 2 with 40% of nodes damaged; Intensity 3 with 60% of nodes damaged. We generate 100 disruptive events for each intensity and assume that the repair time of damaged components with extensive and complete damage follows normal distributions. Their mean values and standard errors refer to the "HAZUS Technical Manual" [65].

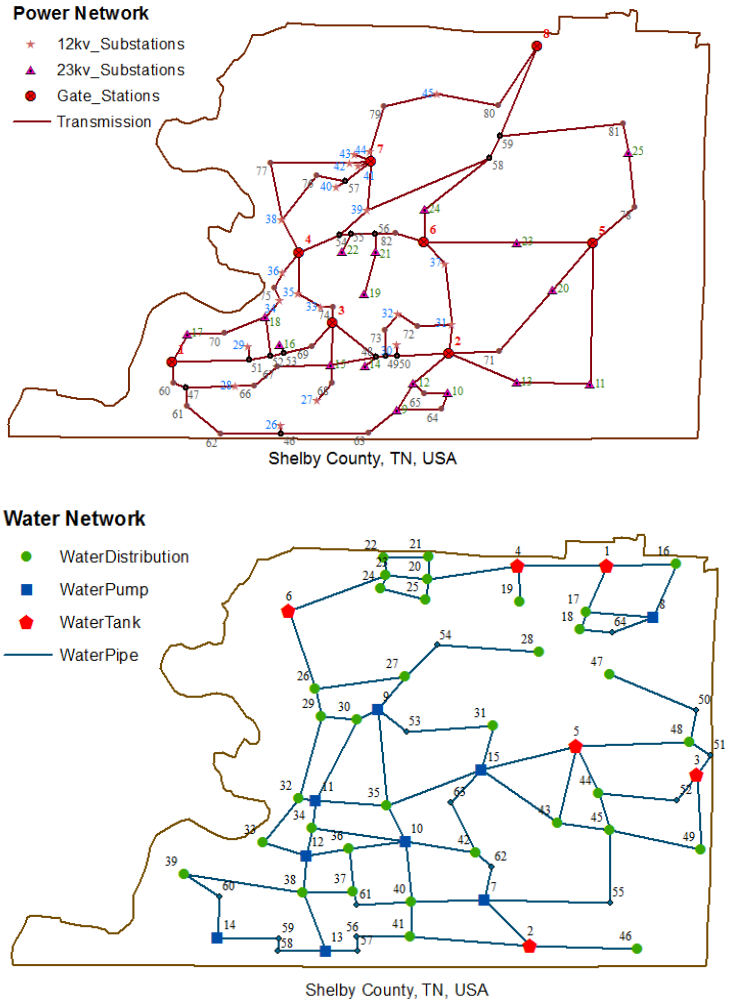

Fig. 9 The layout of the electric power system and water supply system of Shelby County, TN, USA.

For comparison, we introduce two typical methods proposed in the literature: greedy and genetic algorithms. The performance of these three methods is evaluated from solution quality and computational time perspectives. The greedy algorithm determines the repair sequence of damaged components one-by-one and seeks one unrepaired component at each step that can achieve the most considerable benefit. Two factors are considered in this algorithm: the increased integrated system functionality

and the required repair time. The ratio of these two factors measures the benefit of selecting a component. The total number of iterations for this greedy algorithm is I and the number of times to calculate the integrated system functionality is $\frac{I\times(I+1)}{2}$. In the genetic algorithm, a population consists of multiple individuals, and a genotype characterizes each individual and denotes a repair sequence. This method generally contains four steps: 1) generate an initial population; 2) evaluate the fitness value of each repair sequence based on a fitness function; 3) produce the next-generation individuals by the selection, crossover, and mutation operators; 4) repeat steps 2 and 3 until reaching the maximum number of generations. This article sets the number of individuals and the maximum number of generations to 50 and 100, respectively. Furthermore, for the heuristic method, the maximum number of components that can be repaired at each iteration is 10 (i.e., $Q^{max} = 10$).

Moreover, Fig. 10 illustrates the complementary cumulative distribution curves for the relative error produced by three methods under each type of intensity. The optimal repair sequence and its resilience loss are pretty hard to obtain, especially for large-scale systems and disruptive events. The minimal value of the resilience losses provided by these three methods is utilized as the benchmark to evaluate the solution quality of these three methods. Under intensity 1, 55% of disruptive events produced by the heuristic method is larger than 0.1%, and the relative error of all disruptive events is less than 10%. Moreover, the heuristic method can provide the repair sequence with minimal resilience loss for almost all disruptive events under Intensity 2 and 3. As the intensity of the disruptive event increases, genetic algorithm performs worse. The proportion of disruptive events with relative error produced by genetic algorithm less than 0.1 is only 8% and 15% under intensity 1 and 2, while this proportion is increased to 93% under intensity 3. The relative errors produced by the greedy algorithm are larger than 10% for all disruptive events. Hence, the proposed heuristic method can be applied to guide the restoration decision problem of ICISs under different decision-making environments and large-scale disruptions.

Table 2 displays the average resilience loss and computation time produced by these three solution methods over 100 disruptive events for each type of intensity. Although the computational time is less than 60 seconds, the greedy algorithm shows the worst performance in terms of solution quality. The resilience loss provided by the greedy algorithm is, on average, 1.48, 1.64, and 1.68 times that of the heuristic method under Intensity 1, 2, and 3, respectively. Genetic algorithm performs similarly to the proposed heuristic method under Intensity 1 and 2, but it takes much more time than the other two methods (around 40 minutes). In addition, the resilience loss produced by genetic algorithm is, on average, 1.19 times that of the heuristic method under Intensity 3. The proposed heuristic method performs best among these three methods as the average resilience loss is the minimum under all types of intensities, and the computation time is around 30 seconds.

Moreover, Fig. 10 illustrates the complementary cumulative distribution curves for the relative error produced by three methods under each type of intensity. The optimal repair sequence and its resilience loss are pretty hard to obtain, especially for large-scale systems and disruptive events. The minimal value of the resilience losses provided by these three methods is utilized as the benchmark to evaluate the solution quality of these three methods. Under intensity 1, 55% of disruptive events produced by the heuristic method is larger than 0.1%, and the relative error of all disruptive events is less than 10%. Moreover, the heuristic method can provide the repair sequence with minimal resilience loss for almost all disruptive events under Intensity 2 and 3. As the intensity of the disruptive event increases, genetic algorithm performs worse. The proportion of disruptive events with relative error produced by genetic algorithm less than 0.1 is only 8% and 15% under intensity 1 and 2, while this proportion is increased to 93% under intensity 3. The relative errors produced by the greedy algorithm are larger than 10% for all disruptive events. Hence, the proposed heuristic method can be applied to guide the restoration decision problem of ICISs under different decision-making environments and large-scale disruptions.

Table 2

Average resilience loss and computational time of these three solution methods over 100 disruptive events under three types of intensities.

Intensity	Greedy algorithm		Genetic algorithm		Heuristic method	
	Avg. $\mathcal{RL}$	Avg. Time (s)	Avg. $\mathcal{RL}$	Avg. Time (s)	Avg. $\mathcal{RL}$	Avg. Time (s)
1	18.83	7.84	13.05	2464.78	12.72	28.51
2	52.87	17.64	34.52	2541.62	32.16	30.20
3	116.85	41.48	82.55	3699.66	69.54	33.79

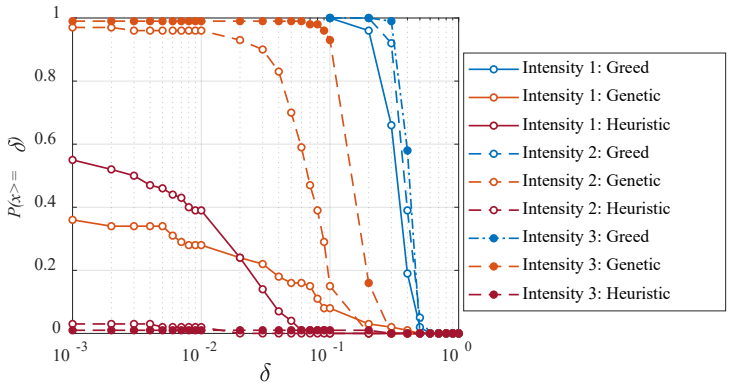

Fig. 10 Complementary cumulative distribution curves for the relative error produced by three methods under each type of intensity.

5.3 Application of the heuristic method under uncertainty

This section illustrates that the proposed heuristic method can be applied to the restoration decision problem in the decision-making environment under uncertainty. This section takes the interdependent system in Section 5.2 as the case system. Taking a disruptive event under intensity 1 as an example, we generate 1000 scenarios to represent the uncertain repair time of damaged components and utilize the proposed heuristic method to calculate the repair sequence. Based on this repair sequence, we can obtain the expected system functionalities at a series of time points and plot the expected restoration curve under this disruptive event in Fig. 11. The upper and lower boundary of the grey-shaded area represent the maximum and minimum values among the 1000 scenarios. Additionally, the required time to restore the system functionality to the pre-disaster level varies, and the maximal and minimal time is 240 days and 90 days, respectively. The computational time for the heuristic method to calculate the repair sequence is around 42 seconds.

To further demonstrate the application of the proposed method in the decision-making environment under uncertainty, this article utilizes this method to calculate the repair plans of 100 disruptive events under each type of intensity in section 5.2. We also generate 1000 scenarios for each disruptive event based on the associated normal functions. Table 3 shows the average expected resilience loss and computational time over these 100 disruptive events under two decision-making environments. Results indicate that the average expected resilience loss under uncertainty is larger than that under certainty. The cause of this situation is that the decision-makers should balance all possible scenarios and then make a feasible and efficient repair plan to cope with the uncertainties. Also, the time required for the proposed method under uncertainty is around 36.62, 52.55, and 93.42 seconds, respectively. Hence, the proposed heuristic method is also appropriate to the restoration decision problem in the decision-making environment under uncertainty.

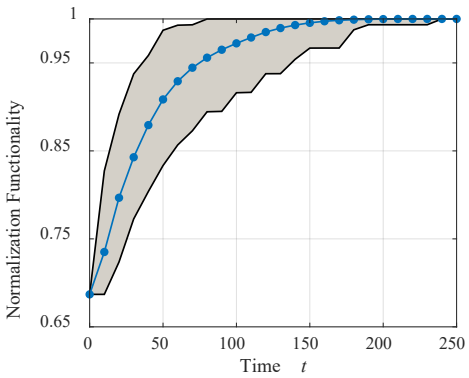

Fig. 11 The expected restoration curve of a disruptive event under intensity 1.

Table 3

Average expected resilience loss and computational time over 100 disruptive events under three types of intensities and two decision-making environments.

Intensity	Decision-making under certainty		Decision-making under uncertainty	
	Avg. $\mathcal{RL}$	Avg. Time (s)	Avg. $\overline{\mathcal{RL}}$	Avg. Time (s)
1	12.72	28.51	13.64	36.62
2	32.16	30.20	35.81	52.55
3	69.54	33.79	76.29	93.42

6. Conclusion

This article studies the post-disaster restoration decision problem of multiple ICISs in the decision-making environment under certainty and uncertainty. First, we establish a resilience-driven deterministic restoration decision model to seek a joint repair sequence that maximizes damaged ICISs' resilience. Physical interdependency is integrated and modeled in this decision model. Next, this article considers the uncertain repair time of damaged components and formulates a two-stage stochastic restoration decision model in the decision-making environment under uncertainty. The first stage seeks an optimum joint repair sequence, and the second stage undertakes operational measures to maximize the weighted resilience value for each scenario under the joint repair sequence. Then, we developed a heuristic method that involves a selection principle and a matrix-based approach to solve the formulated restoration decision models. Finally, a typical case study is presented on two small-scale interdependent systems to illustrate the value of integrating interdependency in the restoration decision problem of disrupted ICISs. The value of the benefit can be up to 30% in some cases. Additionally, we utilize the proposed heuristic method for the post-disaster restoration decision of the interdependent electric power system and water supply system of Shelby County. Results indicate that the heuristic method shows a better performance than the traditional methods in terms of solution quality and computational time; the heuristic method is applicable to the restoration decision problem of ICISs under different decision-making environments and large-scale disruptions; the average computational time is less than 40 and 100 seconds under two decision-making environments with 60% components damaged, respectively.

However, there are still many issues remaining in future directions. Firstly, this article only considers the modeling of repair tasks, but the restoration process involves several tasks, such as fault detection, repair, and commissioning. Hence, we can refer to the rigorous recovery model proposed by Sharma et al. [52] to study the restoration decision problem of ICISs under different decision-making environments. Secondly,

this article utilized resilience loss as the resilience metric, which focuses on the global performance of the joint repair sequence but neglects the disparity in different zones. Hence, incorporating the spatial resilience metrics proposed by Sharma et al. [52], such as the spatial center of resilience and spatial resilience bandwidth, into the restoration decision problem could be a direction for future research. Thirdly, this article only focuses on how to repair damaged components to restore the functionalities of CISs to the pre-disaster level quickly. However, protection actions, such as replacing aging components and expanding system structure, can be implemented to enhance the resistance capacity of infrastructures during the restoration process. Hence, future work will integrate the restoration decision problem with the protection decision problem to further strengthen CISs' resilience. Finally, this article considers physical interdependency among CISs, and the modeling of physical interdependency only captures the satisfied demand of the supporting component. Sharma and Gardoni [66] proposed several functions to model the interdependencies among CISs. Future work can incorporate these functions into the restoration decision problem to formulate a more rigorous mathematical model.

Acknowledgments

This research was jointly supported by the Research Grants Council of the Hong Kong Special Administrative Region (PolyU 15222221), the Project of Strategic Importance (1-ZE0A) and the Department of Civil & Environmental Engineering (WZ06) at the Hong Kong Polytechnic University, Hong Kong. In addition, project 72071174 supported by the National Natural Science Foundation of China at the Hong Kong Polytechnic University Shenzhen Research Institute, Shenzhen, Guangdong, China is gratefully acknowledged.

References

[1] White House (2003) The national strategy for the physical protection of critical

infrastructures and key assets. Available at: https://www.dhs.gov/xlibrary/assets/Physical_Strategy.pdf.

[2] Magoua J J, Li N. The human factor in the disaster resilience modeling of critical infrastructure systems. Reliability Engineering & System Safety, 2023; 232: 109073.

[3] Rinaldi S M, Peerenboom J P, Kelly T K. Identifying, understanding, and analyzing critical infrastructure interdependencies. IEEE control systems magazine, 2001; 21(6): 11-25.

[4] Ouyang M. Review on modeling and simulation of interdependent critical infrastructure systems. Reliability engineering & System Safety, 2014; 121: 43-60.

[5] Vespignani A. The fragility of interdependency. Nature, 2010; 464(7291): 984-985.

[6] Liu X, Fang Y P, Zio E. A hierarchical resilience enhancement framework for interdependent critical infrastructures. Reliability Engineering & System Safety, 2021; 215: 107868.

[7] Muir A, Lopatto J. Final report on the August 14, 2003 blackout in the United States and Canada: causes and recommendations. 2004. Available at: https://www.energy.gov/sites/default/files/oeprod/DocumentsandMedia/BlackoutFinal-Web.pdf.

[8] Sang M, Ding Y, Bao M, Li S, Ye C, Fang Y. Resilience-based restoration strategy optimization for interdependent gas and power networks. Applied Energy, 2021; 302: 117560.

[9] Kumar N, Poonia V, Gupta B B, Goyal M K. A novel framework for risk assessment and resilience of critical infrastructure towards climate change. Technological Forecasting and Social Change, 2021; 165: 120532.

[10] Du A, Wang X, Xie Y, Dong Y. Regional seismic risk and resilience assessment: Methodological development, applicability, and future research needs–An earthquake engineering perspective. Reliability Engineering & System Safety, 2023: 109104.

[11] Wang J, Zuo W, Rhode-Barbarigos L, Lu X, Wang J, Lin Y. Literature review on modeling and simulation of energy infrastructures from a resilience perspective. Reliability Engineering & System Safety, 2019; 183: 360-373.

[12] Liu C, Ouyang M, Wang N, Mao Z, Xu X. A heuristic method to identify optimum seismic retrofit strategies for critical infrastructure systems. Computer-Aided Civil and Infrastructure Engineering, 2021; 36(8): 996-1012.

[13] Eldosouky A R, Saad W, Mandayam N. Resilient critical infrastructure: Bayesian network analysis and contract-based optimization. Reliability Engineering & System Safety, 2021; 205: 107243.

[14] Jansuwan S, Chen A, Xu X. Analysis of freight transportation network redundancy: An application to Utah's bi-modal network for transporting coal. Transportation Research Part A: Policy and Practice, 2021; 151: 154-171.

[15] Fang Y P, Zio E. An adaptive robust framework for the optimization of the resilience of interdependent infrastructures under natural hazards. European Journal of Operational Research, 2019, 276(3): 1119-1136.

[16] Argyroudis S A, Mitoulis S A, Winter M G, Kaynia A M. Fragility of transport assets exposed to multiple hazards: State-of-the-art review toward infrastructural resilience. Reliability Engineering & System Safety, 2019; 191: 106567.

[17] Liu S C, Peng F L, Qiao Y K, Zhang J. Evaluating disaster prevention benefits of underground space from the perspective of urban resilience. International Journal of Disaster Risk Reduction, 2021; 58: 102206.

[18] González A D, Chapman A, Dueñas-Osorio L, Mesbahi M, D'Souza R M. Efficient infrastructure restoration strategies using the recovery operator. Computer-Aided Civil and Infrastructure Engineering, 2017; 32(12): 991-1006.

[19] Zhang C, Kong J, Simonovic S P. Restoration resource allocation model for enhancing resilience of interdependent infrastructure systems. Safety Science, 2018; 102: 169-177.

[20] Çelik M. Network restoration and recovery in humanitarian operations:

Framework, literature review, and research directions. Surveys in Operations Research and Management Science, 2016; 21(2): 47-61.

[21] Zhang Z, Ji T, Wei H H. Dynamic emergency inspection routing and restoration scheduling to enhance the post-earthquake resilience of a highway–bridge network. Reliability Engineering & System Safety, 2022; 220: 108282.

[22] Xu M, Ouyang M, Hong L, Mao Z, Xu X. Resilience-driven repair sequencing decision under uncertainty for critical infrastructure systems. Reliability Engineering & System Safety, 2022; 221: 108378.

[23] Cagnan Z, Davidson R A. Discrete event simulation of the post-earthquake restoration process for electric power systems. International Journal of Risk Assessment and Management, 2007; 7(8): 1138-1156.

[24] Nayak M A, Turnquist M A. Optimal recovery from disruptions in water distribution networks. Computer-Aided Civil and Infrastructure Engineering, 2016; 31(8): 566-579.

[25] Arif A, Ma S, Wang Z, Wang J, Ryan S M, Chen C. Optimizing service restoration in distribution systems with uncertain repair time and demand. IEEE Transactions on Power Systems, 2018; 33(6): 6828-6838.

[26] Fang Y P, Sansavini G. Optimum post-disruption restoration under uncertainty for enhancing critical infrastructure resilience. Reliability Engineering & System Safety, 2019; 185: 1-11.

[27] Iannacone L, Sharma N, Tabandeh A, et al. Modeling time-varying reliability and resilience of deteriorating infrastructure. Reliability Engineering & System Safety, 2022, 217: 108074.

[28] Unal M, Warn G P. A set-based approach to support decision-making on the restoration of infrastructure networks. Earthquake Spectra, 2017; 33(2): 781-801.

[29] Li Q, Roy M, Mostafavi A, Berke P. A plan evaluation framework for examining stakeholder policy preferences in resilience planning and management of urban systems. Environmental Science & Policy; 2021, 124: 125-134.

[30] Li Y, Zhang C, Jia C, Li X, Zhu Y. Joint optimization of workforce scheduling and routing for restoring a disrupted critical infrastructure. Reliability Engineering & System Safety, 2019; 191: 106551.

[31] Liu H, Tatano H, Pflug G, Hochrainer-Stigler S. Post-disaster recovery in industrial sectors: A Markov process analysis of multiple lifeline disruptions. Reliability Engineering & System Safety, 2021; 206: 107299.

[32] Barabadi A, Ayele Y Z. Post-disaster infrastructure recovery: Prediction of recovery rate using historical data. Reliability Engineering & System Safety, 2018; 169: 209-223.

[33] Zhao T, Zhang Y. Transportation infrastructure restoration optimization considering mobility and accessibility in resilience measures. Transportation Research Part C: Emerging Technologies, 2020, 117: 102700.

[34] Wu J, Wang P. Risk-averse optimization for resilience enhancement of complex engineering systems under uncertainties. Reliability Engineering & System Safety, 2021, 215: 107836.

[35] Nurre S G, Cavdaroglu B, Mitchell J E, et al. Restoring infrastructure systems: An integrated network design and scheduling (INDS) problem. European Journal of Operational Research, 2012; 223(3): 794-806.

[36] Vodák R, Bíl M, Křivánková Z. A modified ant colony optimization algorithm to increase the speed of the road network recovery process after disasters. International Journal of Disaster Risk Reduction, 2018; 31: 1092-1106.

[37] Ji C, Wei Y, Mei H, Calzada J, Carey M, Church S, Hayes T, Nugent B, Stella G, Wallace M, White J, Wilcox R. Large-scale data analysis of power grid resilience across multiple US service regions. Nature Energy, 2016; 1(5): 1-8.

[38] Fang Y P, Pedroni N, Zio E. Resilience-based component importance measures for critical infrastructure network systems. IEEE Transactions on Reliability, 2016; 65(2): 502-512.

[39] Liu W, Song Z, Ouyang M, et al. Recovery-based seismic resilience enhancement

strategies of water distribution networks. Reliability Engineering & System Safety, 2020; 203: 107088.

[40] Xu N, Guikema S D, Davidson R A, Nozick L K, Çağnan Z, Vaziri K. Optimizing scheduling of post-earthquake electric power restoration tasks. Earthquake engineering & structural dynamics, 2007; 36(2): 265-284.

[41] Hackl J, Adey B T, Lethanh N. Determination of near-optimal restoration programs for transportation networks following natural hazard events using simulated annealing. Computer-Aided Civil and Infrastructure Engineering, 2018; 33(8): 618-637.

[42] Tan Y, Qiu F, Das A K, Kirschen D S, Arabshahi P, Wang J. Scheduling post-disaster repairs in electricity distribution networks. IEEE Transactions on Power Systems, 2019; 34(4): 2611-2621.

[43] Xu M, Ouyang M, Mao Z, Xu X. Improving repair sequence scheduling methods for post-disaster critical infrastructure systems. Computer-Aided Civil and Infrastructure Engineering, 2019; 34(6): 506-522.

[44] Sun J, Zhang Z. A post-disaster resource allocation framework for improving resilience of interdependent infrastructure networks. Transportation Research Part D: Transport and Environment, 2020; 85: 102455.

[45] Stapelberg R F. Infrastructure systems interdependencies and risk informed decision making (RIDM): impact scenario analysis of infrastructure risks induced by natural, technological and intentional hazards. Journal of systemics, Cybernetics and Informatics, 2008; 6(5): 21-27.

[46] Haimes Y Y, Horowitz B M, Lambert J H, et al. Inoperability input-output model for interdependent infrastructure sectors. I: Theory and methodology. Journal of Infrastructure Systems, 2005; 11(2): 67-79.

[47] Lee II E E, Mitchell J E, Wallace W A. Restoration of services in interdependent infrastructure systems: A network flows approach. IEEE Transactions on Systems, Man, and Cybernetics, Part C (Applications and Reviews), 2007; 37(6): 1303-1317.

[48] Mao Q, Li N. Assessment of the impact of interdependencies on the resilience of networked critical infrastructure systems. Natural hazards, 2018, 93: 315-337.

[49] Cavdaroglu B, Hammel E, Mitchell J E, Sharkey T C, Wallace W A. Integrating restoration and scheduling decisions for disrupted interdependent infrastructure systems. Annals of Operations Research, 2013; 203(1): 279-294.

[50] González A D, Dueñas-Osorio L, Sánchez-Silva M, Medaglia A L. The interdependent network design problem for optimal infrastructure system restoration. Computer-Aided Civil and Infrastructure Engineering, 2016; 31(5): 334-350.

[51] Almoghathawi Y, Barker K, Albert L A. Resilience-driven restoration model for interdependent infrastructure networks. Reliability Engineering & System Safety, 2019; 185: 12-23.

[52] Sharma N, Tabandeh A, Gardoni P. Regional resilience analysis: A multiscale approach to optimize the resilience of interdependent infrastructure. Computer‐Aided Civil and Infrastructure Engineering, 2020, 35(12): 1315-1330.

[53] Sharkey T C, Cavdaroglu B, Nguyen H, Holman J, Mitchell J E, Wallace W A. Interdependent network restoration: On the value of information-sharing. European Journal of Operational Research, 2015; 244(1): 309-321.

[54] Gomez C, González A D, Baroud H, Bedoya-Motta C D. Integrating operational and organizational aspects in interdependent infrastructure network recovery. Risk Analysis, 2019; 39(9): 1913-1929.

[55] Garay-Sianca A, Pinkley S G N. Interdependent integrated network design and scheduling problems with movement of machines. European Journal of Operational Research, 2021; 289(1): 297-327.

[56] Morshedlou N, Barker K, González A D, Ermagun A. A heuristic approach to an interdependent restoration planning and crew routing problem. Computers & Industrial Engineering, 2021; 161: 107626.

[57] Zou Q, Chen S. Enhancing resilience of interdependent traffic-electric power

system. Reliability Engineering & System Safety, 2019; 191: 106557.

[58] Alkhaleel B A, Liao H, Sullivan K M. Model and solution method for mean-risk cost-based post-disruption restoration of interdependent critical infrastructure networks. Computers & Operations Research, 2022, 144: 105812.

[59] Poulin C, Kane M B. Infrastructure resilience curves: Performance measures and summary metrics. Reliability Engineering & System Safety, 2021, 216: 107926.

[60] Sharma N, Tabandeh A, Gardoni P. Resilience analysis: A mathematical formulation to model resilience of engineering systems. Sustainable and Resilient Infrastructure, 2018, 3(2): 49-67.

[61] McCormick G P. Computability of global solutions to factorable nonconvex programs: Part I—Convex underestimating problems. Mathematical Programming, 1976, 10(1): 147-175.

[62] Birge J R, Louveaux F. Introduction to stochastic programming. Springer Science & Business Media, 2011.

[63] Chang S E. Estimation of the economic impact of multiple lifeline disruption: Memphis light, gas and water division case study. NCEER-96-0011, 1996.

[64] Weedy B M, Cory B J, Jenkins N, Ekanayake JB, Strbac G. Electric power systems. John Wiley & Sons, 2012.

[65] FEMA (Federal Emergency Management Agency), HAZUS technical manual, 2003. Retrieved from: www.fema.gov/plan/prevent/hazus.

[66] Sharma N, Gardoni P. Mathematical modeling of interdependent infrastructure: An object-oriented approach for generalized network-system analysis. Reliability Engineering & System Safety, 2022, 217: 108042.